

# Quantifying tempered glass layer compositions using Micro-XRF

Application Note

By Jeff Gelb & Xiaolin Yang | Sigray, Inc

## Abstract

Three different tempered glasses designed as smartphone screen protectors were compared based on elemental composition. Although the glasses were each reported by their manufacturers to have the same hardness values of 9H on the Mohs scale, the glasses varied in their compositional profiles due to differences in their proprietary manufacturing strategies. The three specimens were characterized using the Sigray AttoMap™ micro-XRF, with particular interest in the spatial distribution of potassium and calcium (diffused strengthening elements) in the silicon-rich bulk. 2D surface mapping at <math><5\ \mu\text{m}</math> steps revealed local concentrations of calcium where modification did not complete, and 1D profiling along cross-sections provided insight on the layer design. These results highlighted the similarities and differences between manufacturers in the design of high-hardness tempered glass.

## Introduction

Silicate glasses have been in use for millennia within engineering applications. With archeological relics dating back to the Stone Age, natural glasses have been prized for everything from cutting tools to tableware, and glass artifacts have been found throughout every notable age in history. While prized for optical transparency, unmodified glasses are historically fragile and sensitive to impact and scratching, rendering them inadequate for conditions where impact is anticipated.

Modern glasses are often designed with material additives that strengthen the bulk through a process of chemical modification. The modifications are achieved by exposure to a potassium salt and heat, which leads to an ion exchange at the specimen surface as sodium ions ( $\text{Na}^+$ ) from the glass are swapped for potassium ions ( $\text{K}^+$ ) in the solution [1]. Diffusive processes propagate this exchange into the bulk silicon-rich glass (Si), modifying the chemical structure and introducing a compression-tension stress gradient from the surfaces into the interior [1]. The result is a material that is highly resistant to scratching and fracture, as internal stress gradients discourage the propagation of microcracks [1]. Increases in mechanical hardness because of this toughening (or tempering) regime can be substantial, with commercial tempered glass routinely available featuring hardness values up to 9H on the Mohs scale (similar to that of silicon carbide or tungsten carbide).

As the toughening process is governed by diffusion, it has multiple degrees of freedom. Among them, the processing time, processing temperature, and salt composition have been shown to be particularly influential on the final properties of the tempered glass [1-2]. While the salt treatment is typically a potassium nitrate solution, the addition of calcium has been shown to further enhance mechanical properties; however, when the Ca concentration is too high, the mechanical properties begin to decrease again [2]. Thus, tempering is a delicate endeavor, involving carefully-engineered processes to optimize the hardness and scratch/fracture resistance of the product. Understanding the compositional profile of the material is paramount toward characterizing the diffusion process, which is, in turn, highly beneficial for

better understanding the engineering parameters for optimizing mechanical properties.

In this study, the research aim was to evaluate three different tempered glasses from three different manufacturers, to characterize and ultimately better understand the diffusion gradient resulting from different tempering procedures. The technique of micro X-ray fluorescence (micro-XRF) was used to perform compositional imaging to compare both the localized compositions and global elemental gradients. A quantitative comparison between products was achieved, highlighting the different processes and formulations.

## Method

The present study used a Sigray AttoMap micro-XRF spectrometer. The AttoMap system incorporates patented advancements in X-ray source and optical technologies, providing spatially-resolved analysis to single microns and elemental sensitivity in the sub parts-per-million regime. Samples used in this investigation were commercially-sourced mobile phone screen protectors, which were analyzed along the machined edge to characterize their elemental profiles in cross section. X-ray fluorescence was selected as the technique of choice because it reduces the influence of surface-specific features and contaminants. Furthermore, the charge-neutral properties of X-ray photons eliminate the charging issues of electron-based techniques on bulk insulators, such as glasses, enabling accurate analysis without extensive sample preparation. Figure 1 shows optical micrographs of the exposed cross section of each specimen in the analysis, with each specimen coded as 1-DT, 2-GG, and 3-HG, respectively.

The X-ray source in this study was configured with a copper (Cu) target, operating at 50 kV. A smaller region of 50  $\mu\text{m}$  wide was analyzed across the entire cross section of specimens 1-DT and 2-GG, collecting data in steps of 5  $\mu\text{m}$ . For specimen 3-HG, the analysis was performed across a larger 800  $\mu\text{m}$  width. Peak-fitting and background subtraction routines were subsequently employed on each dataset to reduce noise and enable accurate quantification.

# Quantifying tempered glass layer compositions using Micro-XRF

By Jeff Gelb & Xiaolin Yang | Sigray, Inc

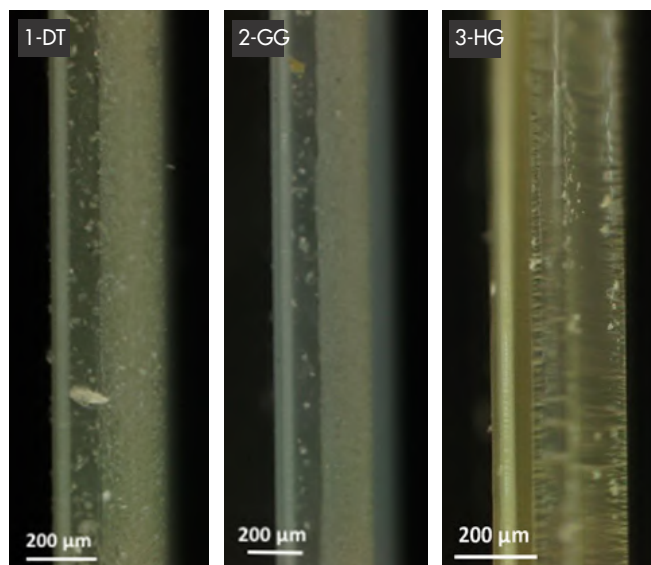


Figure 1. Optical micrographs of the tempered glass cross sections: 1-DT, 2-GG, and 3-HG

## Results and Discussion

Quantitative analysis of the exposed surface layer of each specimen yielded a comparison of the weight percentages of the primary components in each glass, as tabulated in Table 1. The compositions of the 2-GG and 1-DT specimens showed similar levels of Si, K, and Ca, with trace amounts of Ti, while the 3-HG specimen exhibited a remarkably different composition, adding to this mixture Pt, Sn, and Al. This indicated that the chemistries of 2-GG and 1-DT followed similar design principles, while 3-HG utilized a different approach. These measurements provided bulk information about the specimen, with the option for local concentration measurements via mapping, as described next.

	Si	K	Ca	Ti	Pt	Sn	Al
1-DT	97.27	2.49	0.14	0.08	-	-	-
2-GG	96.71	3.09	0.15	0.05	-	-	-
3-HG	79.75	6.21	0.18	0.10	1.55	1.23	10.36

Table 1. Weight percentage of elements measured within the bulk of each glass using the fundamental parameters approach. 1-DT and 2-GG are measured to have similar compositions, while 3-HG exhibits a different composition.

Local elemental mapping with the AttoMap successfully revealed the composition at various points throughout the cross section of each specimen. Figure 2 shows the “heat maps” of the elemental distribution of Si, K, and Ca across the entire 1-DT cross section with brightness intensity corresponding to concentration levels. Figure 3 shows the same for 2-GG. The general profile of each cross section showed similar elements at similar locations: each appeared to be a multi-layered structure, with a Si-rich layer on one side, followed by a gap, and then a layer containing Si, K, and Ca. Thus, the rightmost section of each map was determined to represent the tempered layer in the multi-layered product and was selected as the focus for subsequent data analysis.

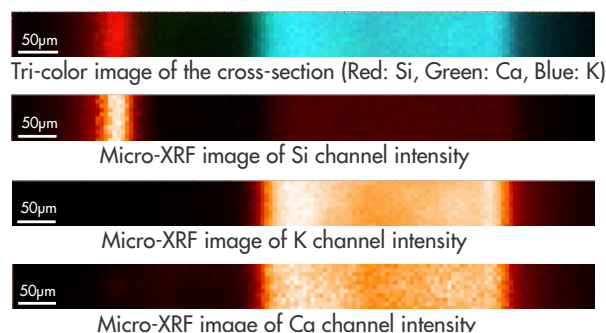


Figure 2. Micro-XRF mapping of the 1-DT cross section. A blended tri-color image is shown, as well as individual contributions from Si, K, and Ca.

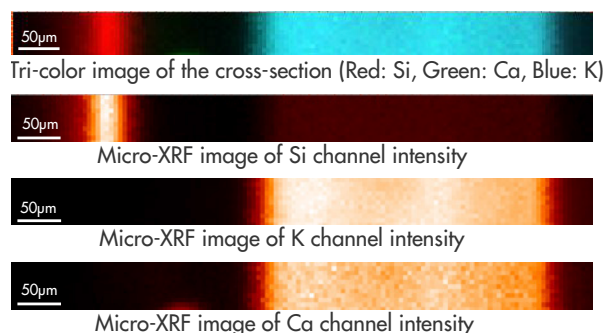
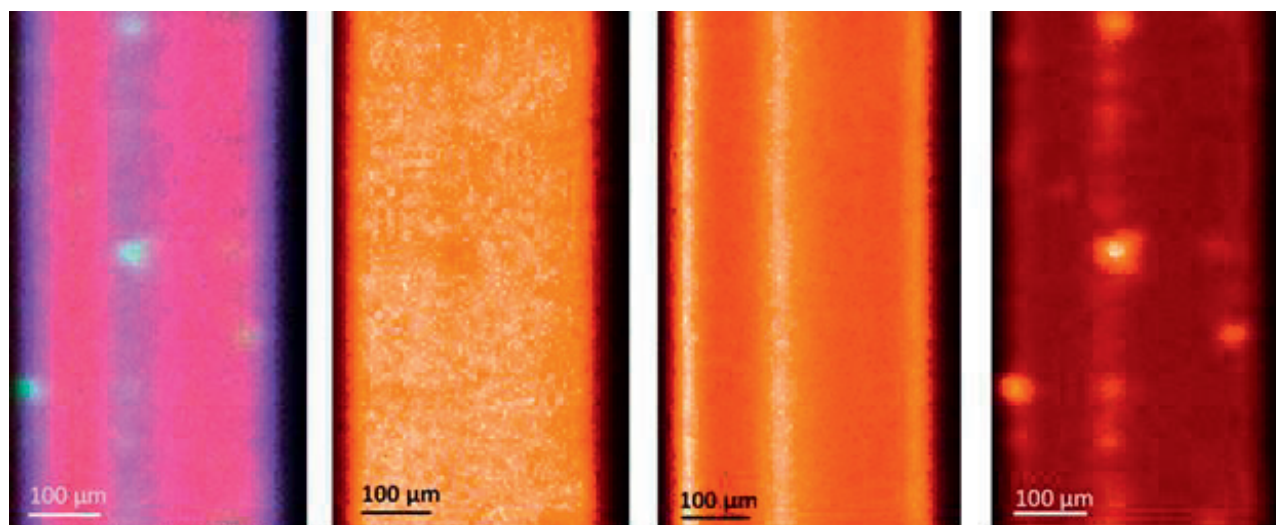


Figure 3. Micro-XRF mapping of the 2-GG cross section.

# Quantifying tempered glass layer compositions using Micro-XRF

By Jeff Gelb & Xiaolin Yang | Sigray, Inc



Tri-color image  
Red: Si, Green: Ca, Blue: K

Micro-XRF image of Si channel

Micro-XRF image of K channel

Micro-XRF image of Ca channel

Figure 4. Micro-XRF mapping of the 3-HG sample.

Examining the 3-HG specimen, some unique features were observed. As shown in Figure 4, some localizations of K and Ca were detected at the two surfaces and midpoint of the volume, which, following similar logic as before, may be assumed to be points of initial contact between Si and K/Ca (e.g., Ca-doped  $\text{KNO}_3$ ). The results would then indicate that the Ca did not diffuse into the bulk of the material in a uniform way (indicated by localized “hot spots” of the Ca signal), pointing toward an incomplete chemical modification in these regions. The K signal was also observed to be high in the center of the diffusion zone and on its edges, similar to 2-GG, which may indicate comparable production strategies between the two glasses.

To better illustrate the global concentration profile of K and Ca, the 2D heat maps were converted to 1D numerical plots. The entire width of each measurement was averaged across the cross-section, converting each 2D map to a corresponding 1D average concentration profile from left to right. These concentration numbers were normalized to their maximum values (within each dataset), providing a quasi-quantitative, numerical comparison between 1-DT, 2-GG, and 3-HG. As shown in Figure 5, the average concentration gradients of Ca and K follow similar trends for each specimen, consistent with the expected behavior of a diffusing species. When, however, the plot is restricted to only the diffusion zone and the primary diffusing species (K), the differences become clearer.

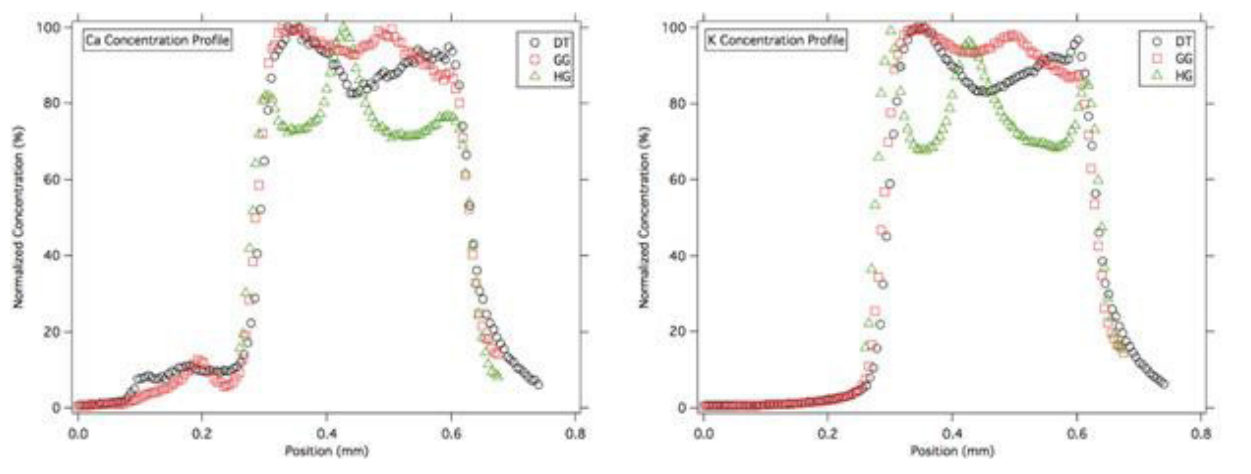


Figure 5. Left graph plots the normalized concentration of Ca and right graph plots the normalized concentration of K for all three samples. Concentration gradients of Ca and K follow similar trends for each specimen and are consistent with expected behavior of a diffusing species.

# Quantifying tempered glass layer compositions using Micro-XRF

Application Note

By Jeff Gelb & Xiaolin Yang | Sigray, Inc

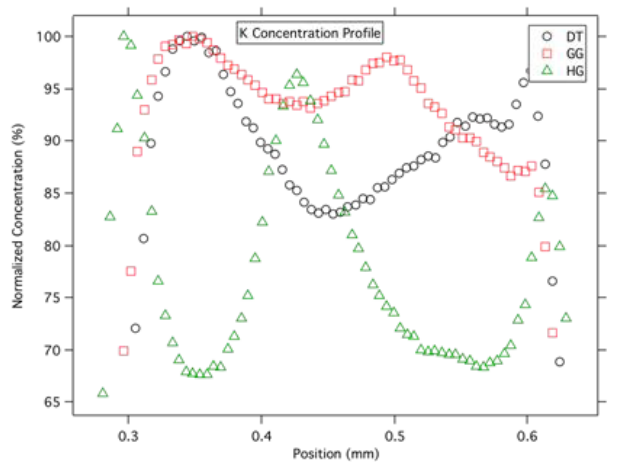


Figure 6. Zoom-in of the plot of potassium (K) within the diffusion zone to more clearly show the spatially-resolved variation in K concentration as a function of position. 1-DT has a single peak in concentration, while 2-GG and 3-HG have two periods

This view, shown in Figure 6, reveals the two “periods” of K concentration in 2-GG and 3-HG, while 1-DT can be seen to more clearly exhibit a single-period profile. These results numerically confirm the visual observations made on the 2D maps, providing a more quantitative insight into the concentration gradients produced by the various fabrication schemes. Similarities between 2-GG and 3-HG suggest that their fabrication strategies may have followed similar principles, while the variant profile observed in 1-DT indicates a different approach.

## Summary

This study demonstrated the utility of Sigray AttoMap microXRF to quantify and characterize compositional variations within different tempered glasses exhibiting similar hardness values. The high, sub-ppm sensitivity and microns-scale resolution of the AttoMap enabled: measurement of trace additives (e.g. Ti); profiling of concentration gradients of low-concentration diffused species; and identification of local regions of incomplete chemical modification. In this study, two glasses exhibited comparable elemental compositions, while the third showed a significantly different approach. By averaging each columnar result to a 1D global concentration profile, similarities and differences in the detected K and Ca content suggested that two glasses may have been tempered through similar protocols, while the third may have used a different approach. All three specimens were reported by their respective manufacturers to have the same hardness values, indicating that different diffusion profiles and fabrication strategies may, nevertheless, lead to similar mechanical properties.

Through the insight provided by the Sigray AttoMap micro-XRF spectrometer, local elemental compositions may be quickly and precisely determined, aiding in a better understanding of diffusion processes used for chemical treatment and mechanical strengthening in commercial glass.

## References

1. R. Gy “Ion exchange for glass strengthening,” *Materials Science and Engineering: B*, vol. 149, no. 2, pp. 159–165, Mar. 2008.
2. V. M. Sglavo, A. Talimian, and N. Ocsko, “Influence of salt bath calcium contamination on soda lime silicate glass chemical strengthening,” *Journal of Non-Crystalline Solids*, vol. 458, pp. 121–128, Feb. 2017.

